Ultrafast Relaxation Dynamics of the Excited States of Michler's Thione

Jahur A. Mondal, Hirendra N. Ghosh, T. Mukherjee, and Dipak K. Palit*

Radiation & Photochemistry Division, Bhabha Atomic Research Centre, Mumbai- 400085, India

Received: April 26, 2006; In Final Form: August 29, 2006

Ultrafast relaxation dynamics of the S_2 and S_1 states of 4,4′-bis(*N*,*N*-dimethylamino)thiobenzophenone (Michler's thione, MT) have been investigated in different kinds of solvents, using steady-state absorption and emission as well as femtosecond transient absorption and fluorescence up-conversion spectroscopic techniques. Steady-state fluorescence measurements, following photoexcitation to the S_2 state of MT, reveal weak fluorescence from the S_2 state ($\phi_F \sim 10^{-3}$ in nonpolar and 10^{-4} in polar solvents) but much weaker fluorescence from the S_1 state. Yield of fluorescence from the S_2 state is reduced in polar solvents because of reduced energy gap between the S_2 and S_1 states, $\Delta E(S_2-S_1)$, as well as interaction with the solvent molecules. Occurrence of S_2-fluorescence in polar solvents, despite small energy gap, suggests that symmetry allowed $S_2(^1A_1) \rightarrow S_0\ (^1A_1)$ radiative and symmetry forbidden $S_2(^1A_1) \rightarrow S_1\ (^1A_2)$ nonradiative transitions are the factors responsible for the S_2 fluorescence in MT. Lifetime of the S_2 state is shorter (varying in the range 0.28−3.5 ps in different solvents) than that predicted from the $\Delta E(S_2-S_1)$ value and this can be attributed to its flexible molecular structure, which promotes an efficient intramolecular radiationless deactivation pathways. The lifetime of the S_1 state (∼1.9−6.5 ps) is also very short because of small energy difference between the S_1 and T_1 states ($\Delta E(S_1-T_1) \sim 300\ cm^{-1}$) in cyclohexane and hydrogen-bonding interaction as well as the presence of the isoenergetic $T_1(\pi\pi^*)$ state to enhance the rate of the intersystem crossing process from the $S_1(n\pi^*)$ state in protic solvents.

1. Introduction

The carbonyl compounds have always been the primary choice for the physical chemists as model compounds for investigation of the fundamental processes of spectroscopy and photochemistry of polyatomic molecules, and as a result, the photophysical and photochemical properties of this class of compounds are well understood.[1−4] During the last three decades, the analogous compounds, in which the carbonyl oxygen atom is replaced by sulfur, selenium or tellurium atom, have also been of special interest to the photochemists and substantial amount of data on the photophysical and photochemical properties of these compounds, particularly those of the sulfur analogues, have been accumulated.[5−12] The C═S bond is weaker than the C═O bond (ca. 430 vs 635 kJ mol^{-1}) and the energy levels of the excited electronic states of the thiocarbonyl compounds occur at lower energies and the spacing between these levels are larger than those in the case of their oxygen analogues.[5] These differences in the properties of the electronic states lead to dramatic differences in the photochemistry and photophysics of these two classes of compounds and many of these properties of the thiocarbonyl compounds are unique in comparison with not only their oxygen analogues but also the organic compounds of other classes.

The following features have been very common in the electronic spectroscopic properties of the thiocarbonyl compounds. The absorption bands corresponding to the $S_1 \leftarrow S_0$, $S_2 \leftarrow S_0$ and even the higher electronic transitions are well resolved in thiocarbonyls.[5,13] In most of the aromatic thiones investigated to date, the S_2 and S_1 states are of $^1(\pi\pi^*)$ and $^1(n\pi^*)$ configurations with $^1A_1$ and $^1A_2$ in C_{2v} symmetries, respectively.[10,14] Because of the large energy gap (typically, in the range 5000−15 000 cm^{-1}) between the S_2 and S_1 states and their different symmetry characters, strong S_2-fluorescence (much stronger than S_1-fluorescence) is a common and regular feature of this class of compounds.[15,16] The $T_1 \leftarrow S_0$ transition is formally electron spin forbidden and is a rare feature in any other class of organic compounds including the carbonyl compounds. However, because of relatively larger spin−orbit coupling owing to a modest "heavy-atom effect" of the S atom (spin−orbit coupling constant of 397 vs 152 cm^{-1} for the O atom), together with the mixing of the $T_1\ ^1(n\pi^*)$ state of $^3A_2$ symmetry with the $T_2\ ^3(\pi\pi^*)$ state of $^3A_1$ electronic symmetry, which are energetically very closely spaced to each other, $T_1 \leftarrow S_0$ transition is a very common feature in the thiocarbonyl compounds.[17,18] In addition, because of very small energy gap between the S_1 and T_1 states (typically in the order of a few hundred inverse centimeters), the $T_1 \leftarrow S_0$ absorption band appears as a weak shoulder or a vibronic structure of the $S_1 \leftarrow S_0$ absorption band.[6] Due to the same reasons, strong $T_1 \rightarrow S_0$ phosphorescence has been observed in almost all thiocarbonyls, which have the T_1 states of $^3(n\pi^*)$ character, in condensed media even at room temperature.[5−7,19] On the other hand, S_1-fluorescence is very weak and very difficult to identify and characterize because of overlapping of the S_1-fluorescence band with the much stronger phosphorescence band.[5,7]

While these unique photophysical properties of the thiocarbonyl compounds are well documented in the literature, the dynamical aspects of them have been perused only recently by a few groups, and the lifetimes of both the S_2 and S_1 states of the thiocarbonyls have been measured to be in the range of a few picoseconds to a few tens of picoseconds using fluorescence and absorption spectroscopic techniques with picosecond or subpicosecond time-resolution.[6,8−16,19] In many of the simpler

* Author for correspondence. E-mail: dkpalit@apsara.barc.ernet.in. Telephone: 91-22-25595091. Fax: 91-22-25505151/25519613.

10.1021/jp062543m CCC: $33.50
Published on Web 10/12/2006

thiocarbonyls, it has been shown that the major fraction of the population created in the S_2 state undergoes the deactivation pathway, $S_2 \rightarrow S_1 \rightarrow T_1$.[5,6,8,9,20] However, in the case of large thiocarbonyl compounds, because of the very small energy gap between the S_1 and T_1 states (<800 cm^{-1}), the $S_1 \rightarrow T_1$ intersystem crossing (ISC) process has been seen to be much faster than the $S_2 \rightarrow S_1$ internal conversion (IC). Therefore, the lifetime of the S_1 state is much shorter than the S_2 state and in some cases the former could not be detected at all.[5,8,9] Among many other thiocarbonyl compounds, the photophysics of 4*H*-1-benzopyrane-4-thione (BPT) and xanthione (XT) have been investigated extensively using femtosecond fluorescence up-conversion and femtosecond transient absorption spectroscopic techniques.[8,9,15] In the cases of BPT in perfluoroalkane and XT in normal alkane solvents, the energy gaps between the S_2 and S_1 states are 8760 and 7680 cm^{-1}, respectively, whereas the energy gaps between the S_1 and T_1 states are 690 and 740 cm^{-1}, respectively.[5] Therefore, the lifetimes of the S_1 states of BPT and XT have been found to be much shorter than those of their S_2 states. Lorenc et al. have reported a lifetime of 1 ps for the S_1 state and 14 ps for the S_2 state of XT in acetonitrile.[20] In a few other cases, study of the dynamics of the S_1 state has been a difficult task, because of its shorter lifetime than that of the S_2 state.[5]

In the present paper, we report the results of our investigation on the photophysical properties of Michler's thione (MT), which is the sulfur analogue of the well-studied carbonyl compound, Michler's ketone (MK). Except for a few reports on the triplet state properties of MT, to the best of our knowledge, no report is available on the dynamics of the excited singlet states of this compound. We have chosen MT for our study with two objectives. First, MT has a moderate energy gap between the S_2 and S_1 states, which is dependent on the characteristics of the solvents as well as a higher energy gap between the S_1 and T_1 states (1555 cm^{-1}) as compared to those of other large thiocarbonyls, e.g. BPT and XT.[5,19] We hope to provide the solvent dependence of the relaxation dynamics of the excited states of the thiocarbonyl compounds. Second, unlike BPT and XT, MT has a flexible structure as well, like its carbonyl analogue, MK, that promises the possibility of twisted intramolecular charge transfer (TICT) process in the excited states.[21] Therefore, this work promises to apprehend the differences in the dynamics of the excited states of the analogous carbonyl and thiocarbonyl compounds.

2. Experimental Section

MT was purchased from Aldrich Chemical Co. and was used as received. All the solvents used were of spectroscopic grade (Spectrochem, India) and used as received without further purification. Steady-state absorption spectra were recorded using a Shimadzu model UV-160A spectrophotometer. The corrected fluorescence spectra were recorded using a Hitachi model 4010 spectrofluorimeter.

Relaxation processes in the sub-500 ps time-domain were measured using a femtosecond pump−probe transient absorption spectrometer, the details of which has been described else where.[22] The laser system consisted of a Ti:sapphire laser oscillator, which is pumped by a 5 W diode-pumped solid-state laser and produces laser pulses of 50 fs duration and 6 nJ energy at 800 nm. These pulses were amplified in an optical amplifier to generate 70 fs laser pulses of about 300 μJ energy at a repetition rate of 1 kHz using the chirped pulse amplification (CPA) technique. Pump pulses at 400 nm were generated for excitation of the samples by frequency-doubling of one part of the 800 nm output of the amplifier in a 0.5 mm thick BBO crystal and the other part of the amplifier output was used to generate the white light continuum (470−1000 nm) probe in a 2 mm thick sapphire plate. The direction of polarization of the pump light was fixed at the magic angle relative to the polarization of the probe light. Sample solutions were kept flowing through a quartz cell of 1 mm path length. The overall time resolution of the absorption spectrometer was determined to be about 120 fs by measuring the ultrafast growth of ESA for tetraphenylprophyrin in benzene. The effects of temporal dispersion on the time-resolved spectra were also eliminated by determining the position of the zero delay between the pump and probe pulses by monitoring the growth of excited-state absorption (ESA) of tetraphenyl porphyrin in benzene at different wavelength in 470−1000 nm region. The temporal profiles recorded using different probe wavelengths were fitted with up to three exponentially decaying or growing components by iterative deconvolution method using an $sech^2$ type instrument response function with fwhm of 120 fs.

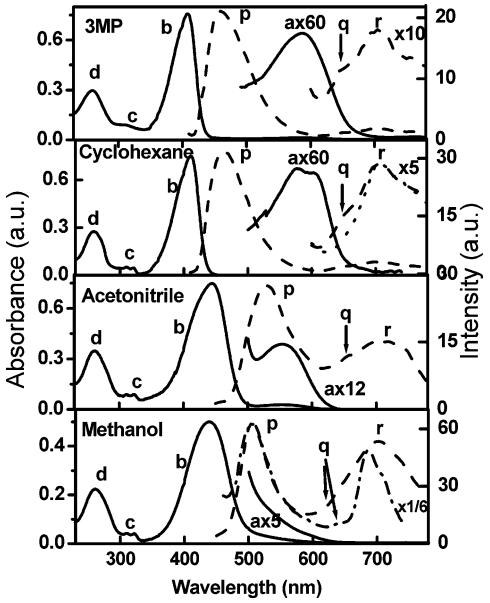

Figure 1. Ground-state absorption, fluorescence and phosphorescence spectra of MT in four different solvents. Bands in the absorption spectra (solid lines and left-hand abscissa) are assigned to $S_1 \leftarrow S_0$ (a), $S_2 \leftarrow S_0$ (b), $S_3 \leftarrow S_0$ (c), and $S_4 \leftarrow S_0$ (d) transitions. Bands in the emission spectra (right-hand abscissa) recorded at room temperature (dashed lines) and in rigid matrixes at 77 K (dash−dotted line) are assigned to $S_2 \rightarrow S_0$ fluorescence (p), $S_1 \rightarrow S_0$ fluorescence (q), and $T_1 \rightarrow S_0$ phosphorescence (r). Emission spectrum presented with dotted line is recorded in cyclohexane using a chopper.

Fluorescence decay profiles for MT in cyclohexane, acetonitrile and methanol have been recorded at 490 and 650 nm using a fluorescence up-conversion spectrometer, which has been described in detail in ref 23. The time resolution of the spectrometer has been determined to be 305 fs.

3. Results

3.1. Steady-State Absorption and Emission Studies. Figure 1 shows the steady-state absorption and emission spectra of MT recorded in four solvents of different polarities and hydrogen-bonding abilities, and Table 1 shows the photophysical and spectroscopic parameters evaluated from them. In each of the aprotic solvents, the absorption spectrum shows four well-resolved absorption bands in the 230−700 nm region. The absorption bands in the 500−700 nm, 350−450 nm, 300−350 nm and 230−300 nm regions are assigned to the $S_1 \leftarrow S_0$,

TABLE 1: Spectroscopic and Photophysical Parameters for MT in Different Solvents[a]

solvent	$S_4 \leftarrow S_0$ transition, λ_{max}, nm ($\bar{\nu}_{max}$, cm^{-1})	$S_2 \leftarrow S_0$ transition, λ_{max}, nm ($\bar{\nu}_{max}$, cm^{-1}) [$E(S_2)$, cm^{-1}]	$S_1 \leftarrow S_0$ transition, λ_{max}, nm ($\bar{\nu}_{max}$, cm^{-1}) [$E(S_1)$, cm^{-1}]	S_2 fluorescence, λ_{max}, nm ($\bar{\nu}_{max}$, cm^{-1}) [SS, cm^{-1}]	S_1 fluorescence, λ_{max}, nm ($\bar{\nu}_{max}$, cm^{-1}) [SS, cm^{-1}]	T_1 phosphorescence, λ_{max}, nm ($\bar{\nu}_{max}$, cm^{-1}) [$E(T_1)$, cm^{-1}]
3MP	260 (38462)	407 (24570) [23419]	585 (17094) [15734]	457 (21882) [2688]	665 (15038) [2056]	715 (13986)
cyclohexane	258 (38760)	409 (24450) [23256]	578 (17301) [15748]	465 (21505) [2945]	668 (14970) [2331]	742 (13477) [15504]
acetonitrile	261 (38314)	443 (22573) [20833]	554 (18051) [16726]	523 (19120) [3453]	660 (15152) [2899]	710 (14085)
methanol	261 (38314)	438 (22831) [20942]	− [17286]	506 (19763) [3068]	645 (15504) [−]	700 (14286) [15385]

[a] $E(S_2)$ and $E(S_1)$ are the energies of the S_2 and S_1 states; SS is the Stokes shift of the S_2 and S_1 fluorescence bands; $\Delta E(S_2-S_1) = 7685$, 7508, 4107, and 3656 cm^{-1} in 3MP, cyclohexane, acetonitrile and methanol, respectively; $\Delta E(S_1-T_1) = 244$ and 1900 cm^{-1} in cyclohexane and methanol, respectively. The error involved in determining the values associated with the S_2 state is about 10% and those associated with the S_1 and T_1 states are about 15%.

$S_2 \leftarrow S_0$, $S_3 \leftarrow S_0$, and $S_4 \leftarrow S_0$ transitions, respectively.[17,18,24−26] The presence of the $T_1 \leftarrow S_0$ band, which is a common feature in the absorption spectrum of many of the thiocarbonyls, is not evident in the absorption spectrum of MT in any kind of solvent.[5] The bands arising due to the $S_1 \leftarrow S_0$ (ϵ(578 nm) ∼ 850 dm^3 mol^{-1} cm^{-1} in cyclohexane) transition is very weak because of the $^1(n\pi^*)$ character of the S_1 state. The intensities of the bands due to the $S_2 \leftarrow S_0$ (ϵ(409 nm) ∼ 5.5×10^4 dm^3 $mol^{-1}cm^{-1}$ in cyclohexane), $S_3 \leftarrow S_0$ (ϵ(312 nm) ∼ 3700 dm^3 $mol^{-1}cm^{-1}$ in cyclohexane), and $S_4 \leftarrow S_0$ (ϵ(256 nm) ∼ 2.0×10^4 dm^3 $mol^{-1}cm^{-1}$ in cyclohexane) transitions are much stronger because of the $^1(\pi\pi^*)$ character of the S_2, S_3 and S_4 states. Hypsochromic and bathochromic shifts of the maxima of the $S_1 \leftarrow S_0$ and $S_2 \leftarrow S_0$ absorption bands in more polar solvents confirm the $^1(n\pi^*)$ and $^1(\pi\pi^*)$ character of the S_1 and S_2 states, respectively. The bathochromic shift is as large as 36 nm (1997 cm^{-1}) in the case of $S_2 \leftarrow S_0$ absorption band in acetonitrile as compared to that in 3MP. This reveals the intramolecular charge transfer (ICT) character of the S_2 state. In the $S_2(\pi\pi^*)$ state, electron charge is partially transferred from the dimethylanilino moieties to the thiocarbonyl group. In methanol, which is a hydrogen-bonding solvent, the maximum of the $S_2 \leftarrow S_0$ absorption band shows a small hypsochromic shift (5 nm) as compared to that in acetonitrile, an aprotic solvent of similar polarity (reaction field parameter, $\Delta F = 0.309$ and 0.312 for methanol and acetonitrile, respectively). In this solvent, the $S_1 \leftarrow S_0$ absorption band too has undergone a large hypsochromic shift to overlap with that arising due to the $S_2 \leftarrow S_0$ transition and the former has appeared only as a long tail to the latter. We do not observe a separate band for the $S_1 \leftarrow S_0$ transition in methanol. Differences in the characteristics of the absorption bands in acetonitrile and methanol possibly arise because of hydrogen-bonding interaction between MT and methanol both in the ground and excited states. A hydrogen-bonding interaction between MT and the methanol molecules is expected to take place at different sites in these two states. In the ground state, the hydrogen bonds are likely to be formed at two nitrogen sites as well as at the sulfur atom site, whereas, in the S_2 state, because of intramolecular charge transfer from the dimethylanilino groups to the thiocarbonyl group, the hydrogen bond energy increases at the sulfur atom site and decreases at the two nitrogen sites. Maciejewski and co-workers reported earlier that photophysics of thioketones are significantly affected by the hydrogen-bonding with the solvent.[8]

Figure 1 also presents the steady-state emission spectra of MT in those four solvents following photoexcitation at 400 nm. As is evident from the absorption spectra, one photon with 400 nm wavelength excites an MT molecule to the higher vibrational levels of its S_2 electronic state. The total emission spectrum recorded in each of these solvents at room temperature apparently consists of two broad bands—one in the 400−600 nm region and another in the 600−800 nm region. In all these solvents, the former fluorescence band, which appears in the energy region higher than that of the $S_1 \leftarrow S_0$ absorption band, can be assigned to the fluorescence emission due to the $S_2 \rightarrow S_0$ radiative transition (we will call it as S_2-fluorescence). The mirror-image relationship between the $S_2 \leftarrow S_0$ absorption and the S_2-fluorescence bands and similarities in the features of the excitation spectrum recorded using 500 nm emission wavelength and those of the $S_2 \leftarrow S_0$ absorption band in each of the solvents support the assignment of the emission band appearing in the 400−600 nm region to the S_2-fluorescence. Quantum yield of S_2-fluorescence, $\phi_F(S_2)$, determined in different solvents are given in Table 2. $\phi_F(S_2)$ decreases significantly in polar solvents as compared to those in nonpolar solvents. Larger bathochromic shift of the S_2-fluorescence maximum and larger Stokes shift in solvents of higher polarity confirm the more polar nature of the emitting S_2 state than that of the ground state. The emission spectrum has also been recorded in rigid matrix of methanol at 77 K. The identical features of the S_2-fluorescence spectra recorded in fluid solution and in rigid matrix suggests that the charge-transfer process taking place in the excited state in polar solvents is not associated with any kind of conformational relaxation, such as twisting of the dimethylamino or dimethylanilino groups.[21,27]

TABLE 2: Yield of S_2-Fluorescence and Lifetimes of Various Relaxation Processes of MT in Different Solvents[a]

solvents (η (cP),[b] ϵ)	$\phi_F \times 10^{-4}$	τ_{S2} (ps)	τ_{S1} (ps)
cyclohexane (0.98, 2.02)	6.8×10^{-4}	3.4	6.2
3MP/*n*-hexane (0.31, 1.89)	6.3×10^{-4} (3MP)	3.1 (*n*-hexane)	4.8 (*n*-hexane)
acetonitrile (0.34, 37.5)	1.4×10^{-4}	0.28	1.9
methanol (0.54, 32.7)	2.3×10^{-4}	0.4[c] 2.2[d]	4.7

[a] Error involved in determination of the fluorescence yield as well as the lifetime values is about 10%. [b] From ref 46. [c] For hydrogen-bonded complex. [d] For non-hydrogen-bonded molecule.

The emission band in the 600−800 nm region is very broad. In nonpolar solvents, its intensity is weaker as compared to that of the S_2-fluorescence band, but increases with increase in polarity of the solvent. In 3MP and cyclohexane, the presence of a shoulder in the higher energy region of this broad emission band is very evident and reveals that the entire band is a combination of two overlapping emission bands occurring in this region. The band appearing as a shoulder to the broad emission band can be assigned to the S_1-fluorescence. The other one, considering the fact that emission of phosphorescence at room temperature is a regular feature of thiocarbonyls, can be assigned to the phosphorescence from the T_1 state (vide infra).[5,6]

In many of the thiocarbonyls, S_1-fluorescence has been characterized as thermally activated delayed fluorescence from the S_1 state.[28] To rationalize the fact whether in this case the S_1-fluorescence band occurred due to normal or delayed fluorescence, we recorded the emission spectrum using the

phosphorescence accessory in the fluorescence spectrometer, which eliminated any short-lived emission component due to normal S_1-fluorescence. We find that, in this spectrum, the shoulder band, which has been assigned to the S_1-fluorescence, vanishes, and only the band due to phosphorescence emission survives. This suggests that the S_1-fluorescence emission observed here is due to normal fluorescence and not due to the delayed fluorescence. Moreover, it also becomes evident that following photoexcitation of MT molecules to the S_2 state, they follow the radiationless deactivation pathway to the T_1 state via the S_1 state (i.e., the pathway $S_2 \rightarrow S_1 \rightarrow T_1$) and not via the T_2 state (i.e., the pathway $S_2 \rightarrow T_2 \rightarrow T_1$), as it was attributed earlier to intersystem crossing to T_2 by a direct spin−orbit coupling mechanism in a few large thiocarbonyls, because of the difficulties in obtaining information about the S_1 state due to their very short lifetime.[5,29]

No attempt has been made to determine the yield of S_1-fluorescence because of several reasons, e.g. very low yield ($\sim 10^{-5}$) as well as strong overlapping of the S_1-fluorescence band with that of phosphorescence. However, the increase in relative intensity of the S_1-fluorescence and phosphorescence emission bands with respect to that of the S_2-fluorescence with increase in polarity of the solvents may be rationalized by the smaller energy gap between the S_2 and S_1 states, which increases the nonradiative $S_2 \rightarrow S_1$ IC process in more polar solvents in compensation of the S_2-fluorescence. In addition, because of stabilization of the $T_2(\pi\pi^*)$ state, it possibly becomes the lowest excited triplet state in polar solvents and hence the $S_1(n\pi^*) \rightarrow T_1(\pi\pi^*)$ ISC process becomes more efficient in polar solvents than the $S_1(n\pi^*) \rightarrow T_1(n\pi^*)$ intersystem crossing process in nonpolar solvents.[30] This is a consequence of El-Sayed's rule.[31]

The hypsochromic shift of the maximum of the phosphorescence band in more polar solvents suggests the $n\pi^*$ character of the T_1 state. However, it is important to note that the widths of the phosphorescence spectra recorded in polar solvents are much larger as compared to those recorded in nonpolar solvents. On the other hand, the width of the phosphorescence spectrum recorded in rigid matrix of methanol at 77 K is much narrower than that recorded in methanol solution at room temperature. These observations possibly can be rationalized by the fact that in nonpolar solvents, the energy of the $^3(n\pi^*)$ state is lower than that of the $^3(\pi\pi^*)$ state and the majority of the phosphorescence emission intensity is of $^3(n\pi^*)$ origin. However, in polar solvents, the $^3(\pi\pi^*)$ state seems to be nearly isoenergetic with the $^3(n\pi^*)$ state and emission from the thermally populated $^3(\pi\pi^*)$ state also contributes to the phosphorescence emission. However, in a rigid matrix of methanol at 77 K, the emission from the $^3(\pi\pi^*)$ state is not observed possibly because either this state is not thermally populated or there is a lack of solvent reorganization (or in other words, incomplete solvation), so this state is not stabilized enough to be isoenergetic with the $^3(n\pi^*)$ state. Another possibility is the presence of different geometrical conformers during phosphorescence emission in solution at room temperature. Most likely, due to the shorter lifetime of the S_2 state in solution, the molecule does not have enough time to undergo conformational changes, and that is why the widths of the S_2-fluorescence recorded in solution at room temperature and in rigid matrix at 77 K are nearly equal, but at a longer time-domain, the molecule in the T_1 state may undergo some kind of conformational changes because of its flexible structure.[21,27]

Energies of the S_2 and S_1 states have been calculated from the intersection point of the corresponding power spectra of the ground-state absorption and fluorescence emissions (i.e., plots of absorbance or fluorescence intensity vs wavenumber (cm^{-1}), which are normalized to the same height). These values are given in Table 1. The electronic energy of the S_1 state in methanol (17268 cm^{-1}) determined in this work agrees well with that (17180 cm^{-1}) determined by Blackwell et al. in ether pentane alcohol glass (17180 cm^{-1}).[25] The values of the energy gaps between the S_2 and S_1 states ($\Delta E(S_2-S_1)$ have also been calculated (see bottom of Table 1). The energy gap decreases in acetonitrile and methanol as compared to those in nonpolar solvents. This is conceivable because the S_2 state with ICT character is more stabilized in more polar solvents, whereas the energy of the S_1 state increases in more polar solvents due to its $n\pi^*$ character. The energy of the $T_1(n\pi^*)$ state could be determined from the onset wavelength of phosphorescence emission on the higher energy side of the phosphorescence spectra in cyclohexane (645 nm or 15504 cm^{-1}) and in methanol (650 nm or 15385 cm^{-1}). Hence, the energy gap between the S_1 and T_1 states ($\Delta E(S_1-T_1)$) have been calculated to be 244 and 1900 cm^{-1} in these two solvents, respectively.

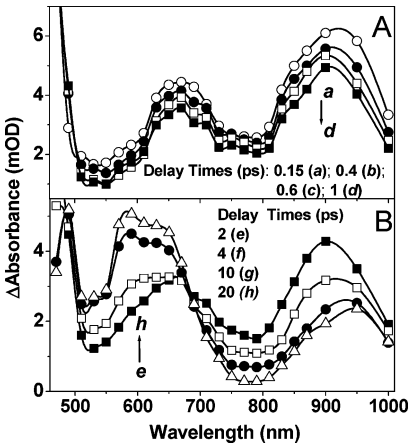

Figure 2. Time-resolved differential absorption spectra of the transients produced following photoexcitation of MT in cyclohexane, using 400 nm light pulses of 70 fs duration.

3.2. Time-Resolved Studies. To explore the dynamics of the S_2 and S_1 states of MT, we performed transient absorption and fluorescence up-conversion studies in subpicosecond time-domain following photoexcitation of MT using 400 nm laser pulses in different kinds of solvents. These two are complementary techniques to reveal the microscopic details of the dynamics of the excited states and the nature of interaction with the solvent.

3.2.1. Transient Absorption Studies. Temporal absorption profiles of the excited states produced following photoexcitation using 400 nm laser pulses of 70 fs have been recorded in a sub-50-ps time-domain with 120 fs time resolution in the 470−1000 nm region at regular intervals of 20 nm and the time-resolved absorption spectra of the transient species have been constructed at different delay times using these data. Figure 2 presents the time-resolved absorption spectra of the transient species produced in cyclohexane. The transient spectrum recorded at 0.15 ps after photoexcitation (spectrum "a" in Figure 2A) has three ESA bands. One of them appears in the 550−750 nm region with maximum at ca. 660 nm, the second one in the 800−1000 nm region with maximum at ca. 870 nm and another in the region below 530 nm, for which the maximum lies at or below 470 nm. The time-resolved spectra constructed in sub-1 ps time-domain show that all the three ESA bands, extending throughout the entire 470−1000 nm region, decay with increase in the delay-time without any significant change in the spectral features (Figure 2A), except for a small

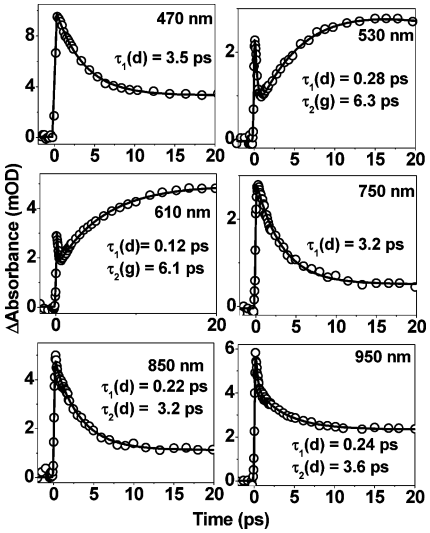

Figure 3. Temporal profiles of the transients monitored at different wavelengths following photoexcitation of MT in cyclohexane along with the best-fit multiexponential function (solid lines). Lifetimes of different components (but not that of the longest component) are shown in the figure. The lifetime of the longest component (500 ps) has been fixed during multiexponential fittings of the temporal profiles using iterative deconvolution method.

hypsochromic shift of the maxima of both the ESA bands observed in the 550−1000 nm region. For example, the maximum appears at ca. 920 nm in the transient spectrum recorded at 0.15 ps and it shifts to 900 nm in that recorded at 1 ps delay-time. However, we observe a significant evolution in the features of the transient spectra recorded when the delay-time is increased from 1 to 20 ps. During this time, ESA continues to decay up to 20 ps in the 700−1000 nm region. On the other hand, ESA increases in the 530−670 nm region in the same time-domain. We also observe the decay of ESA in the 470−500 nm region. As a result, the absorption spectrum recorded at 20 ps delay-time has three ESA bands with maximum at 490, 590, and 950 nm. We find the appearance of a temporary isosbestic point at ca. 680 nm.

Each of the temporal profiles recorded at different wavelengths in the entire 470−1000 nm region follows multiexponential dynamics. Figure 3 presents a few selective ones along with the corresponding multiexponential fit functions. The values of the lifetimes of only the short-lived components ($\tau < 10$ ps) associated with the multiexponential fit functions are given in Figure 3. The lifetime of the longer-lived component (having a lifetime >200 ps), which has been associated with each of the temporal profiles recorded in the said wavelength region, could not be determined accurately using our spectrometer and has not been given in the figures. However, the lifetime of the component associated with the residual absorption observed beyond 20 ps time-domain has been fixed at 500 ps during fitting of the temporal profiles. Each of the temporal profiles monitored in the 800−1000 nm region could be fitted by a triexponential function. In this region, ESA grows initially with the instrument response-time and then decays biexponentially to reach a residual absorption within 20 ps. The lifetimes of two shorter-lived components determined at different wavelengths in this region are nearly same (τ_1(d) = 0.25 ± 0.03 ps, τ_2(d) = 3.4 ± 0.2 ps). However, the relative amplitudes of these three components vary with the monitoring wavelength. This suggests the evolution of more than one kind of transient species absorbing in this spectral region. On the other hand, in the 710−790 nm region, the decay dynamics of ESA could be fitted well with a biexponential decay function with a short-lived component having lifetime, τ_1(d), of 3.4 ± 0.2 ps and another long-lived component, having lifetime >500 ps. In Figure 3, we have presented only the temporal profile recorded at 750 nm as a representative one for this wavelength region.

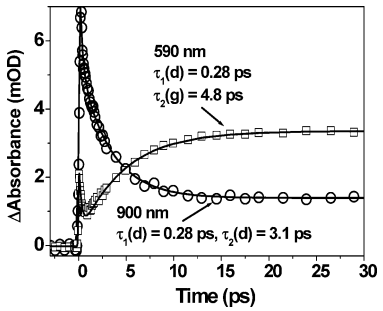

Figure 4. Temporal profiles of the transients monitored at different wavelengths following photoexcitation of MT in *n*-hexane along with the best-fit multiexponential function (solid line). Lifetimes of different components are shown in the insets.

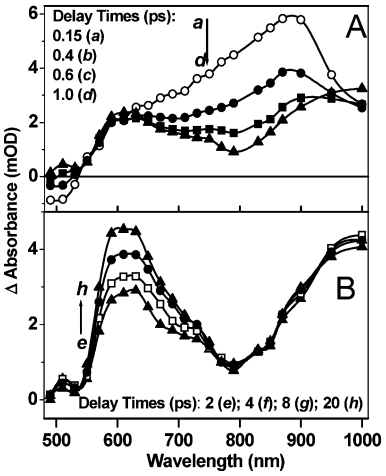

Figure 5. Time-resolved absorption spectra of the transient produced following photoexcitation of MT in methanol, using 400 nm light pulses of 70 fs duration.

However, the temporal profiles recorded in the 470−670 nm region show wavelength-dependent dynamics of the transients, possibly because of overlapping of the ESA bands with any negative absorption band arising due to stimulated emission from the S_2 state, although the differential absorption spectra corresponding to this region do not show the presence of the stimulated emission band. Ground-state bleaching due to photoexcitation may also contribute to the differential absorption signal measured in this wavelength region. Although the temporal dynamics measured at 470 nm is very similar to that observed at 750 nm, each of the temporal profiles recorded in the 510−650 nm region shows the instrument response-time limited rise of ESA, followed by an ultrafast decay and then further growth of ESA to reach a maximum absorbance value. The latter does not decay within 500 ps delay-time. Hence, each of these temporal profiles has been fitted with triple exponential functions. The lifetime of the ultrafast component, τ_1(d), is dependent on the monitoring wavelength, but the lifetime of the growing component, τ_2(g), remains more or less constant (τ_2(g) ~ 6.2 ± 0.2 ps) throughout the wavelength region from 530 to 650 nm. However, the relative amplitudes of all the three components vary with the wavelength. We also investigated the excited-state dynamics of MT in *n*-hexane and the temporal profiles recorded at 610 and 900 nm are shown in Figure 4.

Figure 5 shows the time-resolved absorption spectra of the transient species produced following photoexcitation of MT in

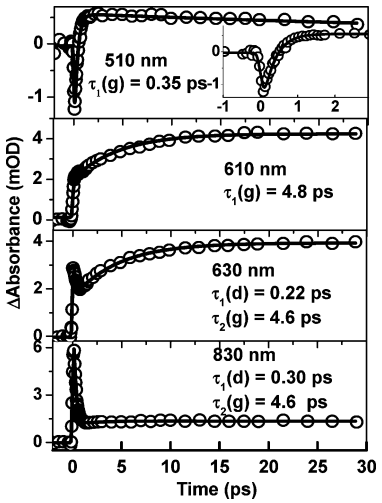

Figure 6. Temporal profiles of the transients monitored at different wavelengths following photoexcitation of MT in methanol along with the best-fit multiexponential function (solid lines). Lifetimes of different components (but not that of the longest component) are shown in the figure. The lifetime of the longest component (500 ps) has been fixed during multiexponential fittings of the temporal profiles using iterative deconvolution method.

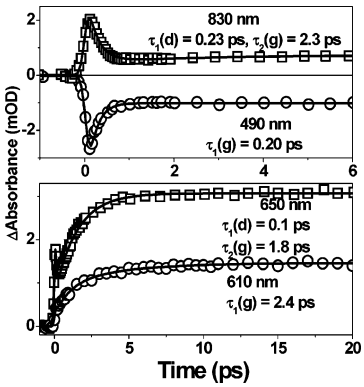

Figure 7. Temporal profiles of the transients monitored at different wavelengths following photoexcitation of MT in ethylene glycol along with the best-fit multiexponential function (solid lines). Lifetimes of different components (but not that of the longest component) are shown in the figure. The lifetime of the longest component (500 ps) has been fixed during multiexponential fittings of the temporal profiles using iterative deconvolution method.

methanol. The transient spectrum constructed for the delay-time of 0.15 ps (spectrum "a" in Figure 5A) shows a negative absorption band in the 490−530 nm region and a broad ESA band in the 550−1000 nm region with a maximum at ca. 870 nm and a shoulder at ca. 630 nm. The negative absorption band may have contribution from either or both of the ground-state bleaching and stimulated emission from the S_2 state, because both the $S_1 \leftarrow S_0$ absorption and as well as the S_2-fluorescence bands occur in this wavelength region (Figure 1). Within the 1 ps delay-time, the negative absorption band decays completely, but not the ESA band. This possibly suggests that the negative absorption band may have arisen due to stimulated emission from the S_2 state (also vide infra). In addition, during this time, ESA band in the 550−1000 nm region evolves due to decrease of absorbance in the 650−950 nm region, but absorbance at wavelengths near the shoulder at 630 nm remains more or less constant. As a result, the spectrum constructed for the delay-time of 1 ps has two ESA bands with maxima at ca. 630 and 1000 nm. Beyond a 1 ps delay-time, the absorbance in the 550−750 nm region increases up to about 15 ps, and no further change is seen up to 500 ps delay-time. However, absorbance in the 750−1000 nm region remains more or less unchanged within 1 to 500 ps delay-times. As a result, the transient spectra recorded at delay-times beyond 15 ps have two ESA bands with maxima at ca. 610 and 1000 nm.

Figure 6 presents the temporal profiles recorded at a few selective wavelengths representing the dynamics associated with the three different bands, namely the stimulated emission band in the 490−530 nm and the ESA bands in the 600−650 nm and 750−1000 nm regions. Temporal dynamics monitored at 510 nm is associated with an ultrafast decay of stimulated emission followed by the rise of a long-lived ESA component, which does not decay appreciably within 500 ps delay-time. The lifetime, τ_1(g), of the process associated with the ultrafast evolution recorded at this wavelength is about 0.35 ps.

The temporal profile recorded at 610 nm shows an initial growth of ESA with the instrument response-time followed by another growing component, having growth lifetime, τ_1(g), of 4.8 ps, to form the long-lived component of ESA. However, the temporal profile recorded at 630 nm reveals the presence of an additional ultrafast decay component of ESA having decay lifetime, τ_1(d), of 0.25 ps, before the ESA grows further with the lifetime, τ_2(g), of 4.6 ps. The temporal profiles recorded at all other wavelengths in the 650−1000 nm region reveal the presence of the same ultrafast decay component having lifetime, τ_1(d), of 0.30 ± 0.05 ps and the component for growing ESA having the growth lifetime, τ_2(g), of 4.5 ± 0.3 ps, as well as the long-lived component of ESA. However, the relative amplitudes of the different components vary with the monitoring wavelength, suggesting the involvement of more than one transient species formed consecutively. We also investigated the excited state dynamics of MT in ethylene glycol, a highly viscous alcoholic solvent and the temporal profiles recorded at a few wavelengths are shown in Figure 7.

We made efforts to study the dynamics of the excited states of MT in acetonitrile. However, due to very quick degradation of the samples following photoexcitation, no meaningful data could be collected in this solvent. Earlier studies on the photophysical properties of thiocarbonyl compounds reveal that acetonitrile is an efficient quencher for the excited states of these molecules. The quenching process in acetonitrile is accomplished by hydrogen abstraction reaction and S_2-exciplex formation.[9,20] However, we have not been able to characterize the MT-solvent exciplex.

3.2.2. Time-Resolved Fluorescence Measurement. We have recorded the fluorescence decay profiles at 490 and 650 nm following photoexcitation of MT in cyclohexane, acetonitrile and methanol using femtosecond fluorescence up-conversion technique. These emission profiles are shown in Figure 8, along with the best multiexponential fit functions. Examination of the steady-state emission spectra of MT in these solvents reveals that the emission profiles recorded at 490 nm provide information regarding the dynamics of the S_2 state, while that recorded at 650 nm may have contribution from the S_1-fluorescence and T_1-phosphorescence as well as the S_2-fluorescnce. The contribution of the latter is expected to be significant in acetonitrile and methanol.

In all the solvents, the intensity of S_2-fluorescence recorded at 490 nm follows instrument response time (305 fs) limited growth. In cyclohexane, S_2-fluorescence decays biexponentially with the lifetimes of 0.28 and 3.7 ps. On the other hand, the fluorescence intensity recorded at 650 nm, following instrument response time-limited growth, decays triexponentially with the two of the components having lifetimes of 0.8 and 6.1 ps and

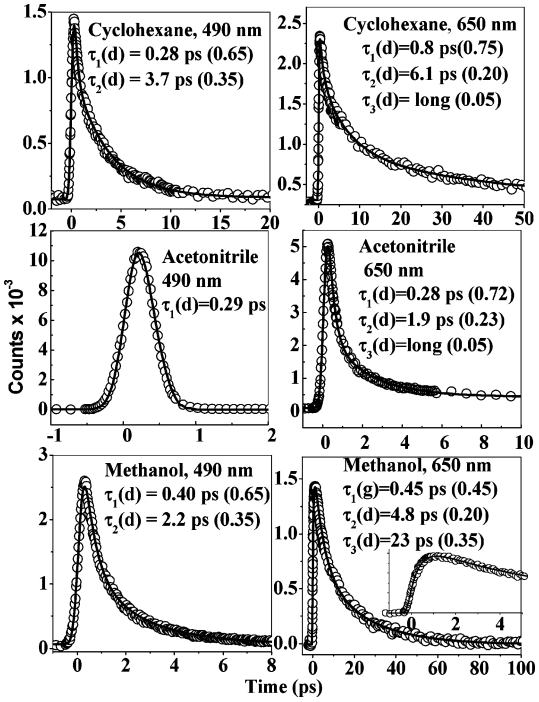

Figure 8. Fluorescence decay profiles of MT in cyclohexane, acetonitrile and methanol recorded at 490 and 650 nm following photoexcitation at 400 nm using fluorescence up-conversion technique. Solid curves represent the best fit with the convolution of the instrument resolution time.

a long-lived component (lifetime is longer than a few hundred picosecond). The decay profile of the S_2-fluorescence in acetonitrile is a Gaussian-like function, which could be fitted with a fluorescence component growing with an instrument response time and an extremely short decay component with lifetime of about 0.29 ps. Again the emission decay profile recorded in the same solvent at 650 nm, after the instrument limited rise, decays triexponentially with lifetimes of 0.28 and 1.9 ps and a long-lived one. In methanol, the decay of S_2-fluorescence at 490 nm, like that in cyclohexane, is biexponential with the lifetimes 0.40 and 2.2 ps. However, the emission decay profile recorded in methanol at 650 nm grows initially with a growth lifetime of 0.45 ps and then decays biexponentially with the lifetimes of 4.8 and 23 ps. Average values of the lifetimes of the S_2 and S_1 states are given in Table 2.

4. Discussion

Our steady-state absorption and emission measurements in solutions at room temperature and in rigid matrix at 77 K establish the fact that upon photoexcitation to its S_2 or higher excited singlet states, MT shows dual fluorescence behavior as well as phosphorescence emission even at room temperature in all kinds of solvents. We mentioned earlier that these occurrences of S_2-fluorescence and room-temperature phosphorescence emission are common features in the case of thiocarbonyl compounds. S_2-fluorescence in thiocarbonyls has been rationalized by the large energy gap between the S_2 and the S_1 states ($\Delta E(S_2-S_1) > 5000$ cm^{-1}). The results of numerous experimental and theoretical studies have revealed that the anomalous S_2-fluorescence, in general, may appear if the $S_2 \rightarrow S_1$ radiationless IC process is sufficiently slowed.[32] The possibility of its occurrence depends mainly on the interplay of two factors, namely, the energy gap between the S_2 and S_1 states and the density of vibrational levels in these two electronic states.[33] The most important factor, due to which the S_2-fluorescence becomes the reality, is the large energy gap between the S_2 and S_1 states.[34] In molecules with the large energy gap between the S_2 and S_1 states, the density of coupled vibrational levels in the S_1 state, which act as accepting modes for the nonradiative energy released by the S_2 state, decreases.[35] Hence the rate of the $S_2 \rightarrow S_1$ IC process becomes slow, resulting longer lifetime of the S_2 state and higher yield of the S_2-fluorescence. The anomalous fluorescence from the S_2 state has been observed in several molecules, in which the value of $\Delta E(S_2-S_1)$ lies in the range 3000−16000 cm^{-1}.[36−38]

In the case of MT, the value of $\Delta E(S_2-S_1)$ is 7685 cm^{-1} in 3MP, but reduces significantly to 4107 and 3656 cm^{-1} in acetonitrile and methanol, respectively (Table 1). Hence, the value of $\Delta E(S_2-S_1)$ is quite moderate in polar solvents to observe the anomalous S_2-fluorescence. Diphenylacetylene is a unique polyene molecule, which shows dual fluorescence in the gas phase despite the small value of $\Delta E(S_2-S_1)$ (∼288 cm^{-1}).[39] Longer lifetime of the S_2 state of this molecule could be explained as a result of a sparse level density of the accepting mode for the $S_2 \rightarrow S_1$ IC process. This hypothesis has been supported by a large temperature dependence of the S_2-fluorescence intensity.[33,35] Recently, we investigated the S_2-fluorescence in a ketocyanine dye (KCD), 2,5-bis[(2,3-dihydroindolyl)propylene] cyclopentanone, for which the energy gap between the S_2 and S_1 states is around 3500 cm^{-1}. In this molecule, S_2-fluorescence could be observed in all kinds of solvents only in rigid matrixes at 77 K.[40] Nonobservance of S_2-fluorescence of KCD in room temperature liquids has been explained by the efficient thermally activated $S_2 \rightarrow S_1$ IC process. At 77 K, the thermal activation is not sufficient to deactivate the major fraction of the population of the S_2 state via the $S_2 \rightarrow S_1$ IC process and hence the rate of radiative decay due to $S_2 \rightarrow S_0$ transition becomes comparable to the former. In the case of MT too, we observe about a 6-fold increase in the intensities of both S_2-fluorescence as well as phosphorescence, but not in S_1 fluorescence, in a rigid matrix of methanol at 77 K. Hence, the occurrence of S_2-fluorescence can be assigned to the reduced $S_2 \rightarrow S_1$ IC process because of weak vibrational coupling between the S_2 and S_1 states.

Apart from the large energy gap and weak vibrational coupling between the S_2 and S_1 states, which may be the prime factors for the slower rate of the $S_2 \rightarrow S_1$ IC process, symmetry restriction and spin multiplicity rules too impose their own efficiency factors.[41,42] Symmetry forbidden transition between the $S_2(^1A_1)$ and $S_1(^1A_2)$ states but symmetry allowed radiative transition between the $S_2(^1A_1)$ and $S_0(^1A_1)$ states may be the responsible factors for occurrence of S_2-fluorescence in the case of MT in polar solvents, despite lower energy gap between the S_2 and S_1 states.

It becomes evident from Figure 1 and Table 1 that photoexcitation of MT using 400 nm light (energy = 25 000 cm^{-1} per photon) creates the molecules in the S_2 state with about 1581 and 4058 cm^{-1} of excess vibrational energies in cyclohexane and methanol, respectively. Our time-resolved absorption study in cyclohexane shows that following creation of the S_2 state, ESA decays biexponentially with the lifetimes of 0.25 ± 0.03 and 3.4 ± 0.2 ps (850 and 950 nm profiles in Figure 3). Measurement of S_2-fluorescence also reveals the biexponential decay of the S_2 state with the lifetimes of 0.28 and 3.7 ps. These information along with the similarities in the features of the transient spectra constructed for the delay times of 0.15 and 1 ps are tempting to assign the ultrafast decay lifetime component of about 0.25 ± 0.03 ps to the vibrational energy relaxation in

the S_2 state. However, it is important to note that if the said ultrafast component has arisen due to vibrational relaxation process, we are expected to observe the growth of S_2-fluorescence with the same lifetime instead of the decay component. Hence the assignment of this ultrafast component to the vibrational relaxation process may not be justified. So we propose that the same component may have arisen due to the anti-twisting motion of phenyl groups with respect to the thiocarbonyl group. We have shown earlier that in the ground state of MK, which is an carbonyl analogue of MT, the two phenyl rings of the dimethylanilino groups are at a dihedral angle of 51° with respect to each other because of steric interaction between them. So immediately after photoexcitation, an ultrafast anti-twisting motion may bring back the pre-twisted molecule to a near planar geometry with high mesomeric interaction and intramolecular charge-transfer character.[27] The second component of (3.5 ps) may be assigned to the lifetime of the nearly planar S_2 state. In hexane, the lifetime of the S_2 state is 3.1 ps.

Taking into account the facts that the major deactivation pathway of the S_2 state is the internal conversion process and the value of $\Delta E(S_2-S_1)$ is about 7500 cm^{-1} in cyclohexane, the lifetime of the S_2 state is expected to be about 20 ps, as per the energy gap law.[43] Hence the lifetime of the S_2 state of MT determined here is much shorter than expected from the energy gap law. We calculated the lifetime of the S_2 state using equation, $\tau(S_2) = \phi_f(S_2)/k_f(S_2)$. In this equation, k_f is the radiative rate constant, which can be calculated using the Strickler−Berg equation, eq 1[44]

$$k_f = 2.88 \times 10^{-9} n^2 \langle \bar{\nu}_f^{-3} \rangle^{-1} \int \frac{\epsilon(\bar{\nu}) d(\bar{\nu})}{\bar{\nu}} \qquad (1)$$

where n is the refractive index of the solvent, $\langle \bar{\nu}_f^{-3} \rangle^{-1}$ is the reciprocal of the average value of $\langle \bar{\nu}_f^{-3} \rangle$ over the fluorescence spectrum, $\epsilon(\bar{\nu})$ in the molar extinction coefficient, and the integral is taken over the absorption spectrum. In cyclohexane, the value of ϕ_f is 6.8×10^{-4} (Table 2) and the value of k_f calculated using eq 1 is 2.51×10^8 s^{-1}. Hence, the calculated value of $\tau(S_2)$ is 2.72 ps. This justifies the assignment of the 3.5 or 3.1 ps component in cyclohexane or hexane to the lifetime of the S_2 state. The much shorter lifetime of the S_2 state of MT in these solvents as compared to that of the rigid aromatic thiones can be attributed to its flexible molecular structure, which promotes an efficient intramolecular radiationless deactivaton pathway via the low-frequency internal rotational and out-of-plane bending modes.[5]

We recorded the evolution of the transient absorption spectra up to about 20 ps and the characteristics of the spectra recorded at 20 ps delay-time do not change up to the delay-time of 500 ps. We find that the characteristics of the transient spectrum recorded in cyclohexane at 20 ps delay-time are very similar to those of the triplet−triplet absorption spectrum of MT in benzene reported by Kumar et al. in the 470−750 nm region.[19] From their laser flash photolysis study of MT in benzene, Kumar et al. reported the presence of two ESA bands with maxima at 470 and 610 nm.[19] Hence, the spectrum "h", recorded at 20 ps in either of the solvents (Figures 2B and 5B), can be assigned to the lowest excited triplet (T_1) state of MT, which has a long lifetime (1.3 ms in benzene).[5] Thus, the growth lifetimes of ESA, $\tau_2(g) = 6.2 \pm 0.1$ ps (Figure 3) or 4.8 ps (Figure 4) measured in the 530 or 610 nm region in cyclohexane or hexane can be assigned to the lifetime of the S_1 state of MT.

The time-resolved fluorescence measurement at 650 nm, at which contributions from the fluorescence emissions from both the S_1 and S_2 states as well as the phosphorescence emission from the T_1 state are expected (see Figure 1), shows the nonexponential decay of the emission intensity. The decay profile could be best fitted by a function with at least three exponential terms, with the lifetimes of 0.6 ps, 6.1 ps as well as a long component (>100 ps) with a very small amplitude. Obviously the long component can be assigned to the phosphorescence decay and the component with the lifetime of 6.1 ps to the lifetime of the S_1 state in cyclohexane. This is in agreement with the assignment made from the results of the transient absorption measurements. We cannot explain the presence of the component with lifetime of 0.6 ps, which may have deceptively appeared because of the combination of the biexponential decay of the S_2 state (lifetimes of 0.28 and 3.7 ps) and the growth of the weakly fluorescent S_1 state (lifetime of 3.7 ps) with varying amplitudes. It is true that the nonexponential emission decay profile should be fitted with a function representing the consecutive reaction process $S_2 \rightarrow S_1 \rightarrow T_1 \rightarrow S_0$. However, without the knowledge of the exact values of the quantum yields of the radiative and nonradiative processes from each of these excited states, fitting of the curve using this scheme is an impossible task, and hence, no attempt has been made toward this task.

In polar solvents, the fluorescence quantum yield and lifetime of the S_2 state are smaller as compared to those in nonpolar solvents and this is in agreement with the prediction based on the much lower energy gap between the S_2 and S_1 states (Tables 1 and 2). In acetonitrile, the fluorescence lifetime of the S_2 state has been determined to be about 0.29 ps, while the calculated value is 0.49 ps using the value of k_f (2.86×10^8 s^{-1} from eq 1). Two values are in good agreement. Burdzinski et al. have studied the mechanism and dynamics of the efficient quenching of the S_2 state of bezopyranthione by acetonitrile.[9] They suggested the involvement of two aborted processes in the quenching mechanism: exciplex formation and hydrogen atom abstraction by the solvent. Lorenc et al. reported the formation of S_2-exciplex as an efficient mechanism for the quenching of the S_2 state of xanthione in acetonitrile.[20] We too could not detect any transient species of MT in acetonitrile in transient absorption experiment, because of strong quenching interaction between the S_2 state and the solvent. Time-resolved measurements of the emission decay at 650 nm could be fitted using a triexponential function and following the explanation provided earlier as in the case of cyclohexane, the component with lifetime of 1.9 ps could be assigned to that of the S_1 state.

In methanol, the fluorescence decay monitored at 490 nm could be fitted with two exponentials with the lifetimes of 0.4 and 2.2 ps. If we follow the same arguments as provided in the case of cyclohexane, these must be assigned to those arising due to the relaxation of the S_2 state by an anti-twisting motion followed by the population decay. However, using the ϕ_F value of 2.3×10^{-4} and the calculated value of k_f of 2.82×10^8 s^{-1}, we estimate the lifetime of the S_2 state as 0.82 ps. This value does not agree with the assignment of the lifetime of the S_2 state of 2.2 ps. In the transient absorption experiments, we also observe the decay of stimulated emission monitored at 510 nm with lifetime of 0.35 ps. However, we do not observe the component with lifetime of 2.2 ps in the decay of stimulated emission. Absence of this component may be not so surprising in the case if the stimulated emission decay is accompanied by the growth of ESA due to formation of the S_1 state followed by the decay of the S_2 state. It is also important to note that the transient absorption spectrum recorded at 0.15 ps delay-time in methanol is significantly different from that recorded at 0.15 ps delay-time in cyclohexane (Figures 2A and 5A). All these

facts can possibly be explained by the fact that MT forms hydrogen-bonded complex with methanol in the ground state and both the non-hydrogen-bonded form of MT and the hydrogen-bonded complex, which remain in equilibrium in the ground state, are excited by 400 nm light. Hence, the two components observed in the fluorescence decay profile of the S_2 state can be assigned to the excited states of the hydrogen-bonded complex and the non-hydrogen−hydrogen-bonded form, which have lifetimes of 0.4 and 2.2 ps, respectively (Table 2). The shorter lifetime (2.2 ps) of the non-hydrogen bonded form of the S_2 state in methanol as compared to that in cyclohexane (3.7 ps) is quite justified considering the lower energy gap in methanol as compared to that in cyclohexane. In this solvent, the lifetime of the hydrogen-bonded complex (0.4 ps) is comparable to that arising from the anti-twisting motion observed in cyclohexane.

Emission profile monitored at 650 nm shows an initial growth with a lifetime of 0.45 ps and then it decays biexponentially with the lifetimes of 4.8 and 23 ps. The emission profile at this wavelength should have contributions from the singlet and triplet excited states of both the non-hydrogen-bonded form and hydrogen-bonded complex. So, it becomes clearly evident that the lifetimes of the three components only reveal the average lifetimes, the value of which depends on the values of the corresponding preexponential parameters, for the growth and decay of the S_1 state as well as the decay of the triplet state. In light of this argument, the component with growth lifetime of 0.45 ps can possibly be assigned to the formation of the hydrogen-bonded complex of the S_1 state formed as a result of deactivation of the hydrogen bonded complex of the S_2 state. On the other hand, the decay lifetimes of 4.8 and 23 ps can be assigned to the decay lifetime of the non-hydrogen-bonded and hydrogen-bonded complexes of the S_1 state, respectively. The lifetime of 4.8 ps is in close agreement with the growth lifetime of the ESA signal monitored in the 610−850 nm region (Figure 6) and hence assigned to the growth of the T_1 state. The decay of the lowest triplet state of MT in methanol should be characterized by a lifetime much longer than 23 ps because of its $\pi\pi^*$ character.

MT is a flexible molecule, where the dimethylanilino groups are directly linked to the thiocarbonyl group. Generally, in the case of molecules with flexible structure and electron donating and accepting groups linked together directly or via π-conjugation, twisted intramolecular charge transfer (TICT) is a common process, which determines the relaxation pathways of the excited state.[45,46] It has been well established that in the S_1 state, MK, the carbonyl analogue of MT, undergoes TICT dynamics following photoexcitation.[27] As indicated in the steady-state absorption and emission studies, the S_2 state of MT is more polar as compared to the ground state. Hence, it is interesting to investigate whether TICT dynamics play any role in the relaxation dynamics of the excited state of MT. Since TICT dynamics is expected to slow in solvents of higher viscosity, the lifetime of the excited-state involved in the twisting process should be larger as the viscosity of the solvent is increased. Hence, we investigated the temporal dynamics of the excited states of MT at a few selective wavelengths following photoexcitation of MT in ethylene glycol (Figure 7). Polarity of ethylene glycol (the reaction field parameter, ΔF (= 0.274) of this solvent is nearly equal to that of methanol $\Delta F = 0.309$) but the former (viscosity, $\eta = 26.09$ cP) is about 50 times more viscous than the latter ($\eta = 0.54$ cP) at 298 K.[47]

Analysis of the temporal profiles reveal that, in ethylene glycol (Figure 7) the lifetime of the S_2 state is around 0.22 ps, which is in the range of the lifetime of the hydrogen-bonded complex in methanol. The lifetime of the S_1 state is even shorter (2.2 ± 0.2 ps) in this solvent. The shorter lifetimes of the S_2 and S_1 states in ethylene glycol as compared to those in methanol, despite higher viscosity of the former solvent, may be attributed to stronger hydrogen bonding interaction. This observation suggests that the dynamics of MT in the S_1 state is nearly independent of solvent viscosity and does not follow the TICT mechanism.

Difference in the relaxation dynamics in the excited states of MT and MK can be rationalized by the following argument. Because of lower electro negativity of the sulfur atom (2.5 eV) as compared to that of the oxygen atom (3.5 eV), the thiocarbonyl group (>C═S) is a weaker electron acceptor than that of the carbonyl group (>C═O). This weak electron accepting nature of >C═S is possibly not sufficient to promote the TICT process in MT. Following photoexcitation, the S_2 state quickly decays down to the S_1 state, in which the charge transfer is not a favorable process because of its $n\pi^*$ character. In addition, since the energy gap between the S_1 and T_1 states is much smaller and the spin−orbit coupling is much stronger in MT than that in carbonyl analogues, the ISC process is very efficient and the lifetime of the S_1 state is too short (only a few picoseconds), to allow the twisting process.

To summarize, in this paper, we report the results of our investigation on the photophysical properties of the excited singlet, both the S_2 and the S_1, states of Michler's thione in different kinds of solvents. Steady-state absorption and fluorescence measurements have been used to characterize the fluorescence from the S_2 and S_1 states as well as phosphorescence from the T_1 state of MT in solution at room temperature in all kinds of solvents and rigid matrix of methanol at 77 K. Femtosecond transient absorption spectroscopy and fluorescence up-conversion technique have been used to unravel the relaxation dynamics of the S_2 and S_1 states. The lifetimes of the S_2 and S_1 states are strongly dependent on solvent polarity and proticity. While these values are 3.4 and 6.2 ps in cyclohexane, in acetonitrile they are extremely short-lived with the lifetimes of 0.29 and 1.9 ps, respectively. This is possibly due to strong quenching interaction of the excited states with acetonitrile. In alcoholic solvents, MT forms hydrogen-bonded complex, which remain in equilibrium with the non-hydrogen-bonded form in the ground state. Because of the presence of both these species in the excited states, their dynamics of relaxation have been seen to be more complicated. Unlike in MK, we have not been able to observe the TICT process possibly because of very short lifetimes of the excited singlet states and weak electron accepting ability of the thiocarbonyl group.

Acknowledgment. The femtosecond up-conversion data were recorded at the DST sponsored femtosecond facility at Indian Association for the Cultivation of Science, Kolkata, India. We thank Mr. K. Sahu, Mr. S. K. Mondal, and Prof. K. Bhattacharaya for their kind help in recording the fluorescence up-conversion data.

References and Notes

(1) (a) Wagner, P. J. *Top. Curr. Chem.* **1976**, *66*, 1. (b) Wagner, P. J.; Park, B. S. *Org. Photochem.* **1991**, *11*, 227.
(2) Formosinho, S. J.; Arnaut, L. G. *Adv. Photochem.* **1991**, *16*, 67.
(3) Scaiano, J. C. *J. Photochem.* **1973**, *2*, 81.
(4) Cohen, S. G.; Parola, A.; Parsons, G. H. *Chem. Rev.* **1973**, *73*, 141.
(5) Maciejewski, A.; Steer, R. P. *Chem. Rev.* **1993**, *93*, 67.
(6) Szymanski, M.; Maciejewski, A.; Steer, R. P. *J. Phys. Chem.* **1988**, *92*, 2485.

(7) Szymanski, M.; Maciejewski, A.; Steer, R. P. *Chem. Phys.* **1988**, *124*, 143.
(8) Burdzinski, G.; Maciejewski, A.; Buntinx, G.; Poizat, O.; Toele, P.; Zhang, H.; Glasbeek, M. *Chem. Phys. Lett.* **2004**, *393*, 102.
(9) Burdzinski, G.; Maciejewski, A.; Buntinx, G.; Poizat, O.; Lefumeux, C. *Chem. Phys. Lett.* **2004**, *384*, 332.
(10) Moule, D. C.; Lim, E. C. *J. Phys. Chem. A* **2002**, *106*, 3072.
(11) Emeis, C. A.; Oosterhoff, L. J. *J. Chem. Phys.* **1971**, *54*, 4809.
(12) Englebrecht, J. P.; Anderson, G. D.; Linder, R. E.; Barth, G.; Bunnenberg, E.; Djerassi, C.; Seamans, L.; Moscowitz, A. *Spectrochim. Acta* **1975**, *31A*, 507.
(13) Ramamurthy, V.; Steer, R. P. *Acc. Chem. Res.***1988**, *21*, 380.
(14) Kubicki, J.; Maciejewski, A.; Milewski, M.; Wrozowa, T.; Sreer, R. P. *Phys. Chem. Chem. Phys.* **2002**, *4*, 173.
(15) Burdzinski, G.; Maciejewski, A.; Buntinx, G.; Poizat, O.; Lefumeux, C. *Chem. Phys. Lett.* **2003**, *368*, 745.
(16) Burdzinski, G.; Ziolek, M.; Karolczak, J.; Maciejewski, A. *J. Phys. Chem. A* **2004**, *108*, 11160.
(17) Maki, A. H.; Svejda, P.; Huber, J. R. *Chem. Phys.* **1978**, *32*, 369.
(18) Safarzadeh-Amiri, A.; Verrall, R. E.; Steer, R. P. *Can. J. Chem.* **1983**, *61*, 894.
(19) Kumar, C. V.; Qin, L.; Das, P. K. *J. Chem. Soc., Faraday Trans. 2* **1984**, *80*, 783.
(20) Lorenc, M.; Maciejewski, A.; Ziolek, M.; Naskrecki, R.; Karolczak, J.; Kubicki, J.; Ciesielska, B. *Chem. Phys. Lett.* **2001**, *346*, 224.
(21) Veldhoven, E. von.; Zhang, H.; Rettig, W.; Brown, R. G.; Hepworth, J. D.; Glasbeek, M. *Chem. Phys. Lett.* **2002**, *363*, 189.
(22) Mondal, J. A.; Ramakrishna, G.; Singh, A. K.; Ghosh, H. N.; Mariappan, M.; Maiya, B. G.; Mukherjee, T.; Palit, D. K. *J. Phys. Chem. A* **2004.** *108*, 7843.
(23) Sahu, K.; Mondal, S. K.; Ghosh, S.; Roy, D.; Sen, P.; Bhattacharyya, K. *J. Phys. Chem. B* **2006**, *110*, 1056.
(24) Capitanio, D. A.; Pownall, H. J.; Huber, J. R. *J. Photochem.* **1974**, *3*, 225.
(25) Blackwell, D. S.; Liao, C. C.; Loutfy, R. O.; de Mayo, P.; Paszyc, S. *Mol. Photochem.* **1972**, *4*, 171.
(26) Mahaney, M.; Huber, J. R. *J. Mol. Spectrosc.* **1981**, *87*, 438.
(27) Mondal, J. A.; Ghosh, H. N.; Ghanty, T. K.; Mukherjee, T.; Palit, D. K. *J. Phys. Chem. A* **2006**, *110*, 3432.
(28) Maciejewski, A.; Szymanski, M.; Steer, R. P. *J. Phys. Chem.* **1986**, *90*, 6314.
(29) Molenkamp, L. W.; Weitekamp, D. P.; Wiersma, D. A. *Chem. Phys. Lett.* **1983**, *99*, 382.
(30) Maciejewski, A.; Szymanski, M.; Steer, R. P. *Chem. Phys. Lett.* **1988**, *143*, 559.
(31) El-Sayed, M. A. *J. Phys. Chem.* **1963**, *38*, 2834.
(32) Ermolaev, V. L. *Russ. Chem. Rev.* **2001**, *70*, 471.
(33) Lituinenko, K. L.; Webber, N. M.; Meech, S. R. *J. Phys. Chem. A* **2003**, *107*, 2616.
(34) Foggi, P.; Neuwahl, F. V. R.; Moroni, L.; Salvi, P. R. *J. Phys. Chem. A* **2003**, *107*, 1689.
(35) Nemes, P.; Demeter, A.; Biczok, L.; Bereces, T.; Wintgens, V.; Valat, P. Kossanyi, J. *J. Photochem. Photobiol.* A Chem. **1998**, *113*, 225.
(36) Bachilo, S. M.; Gillbro, T. *Chem. Phys. Lett.* **1994**, *218*, 557.
(37) Eber, G.; Schneider, S.; Doerr, F. *J. Lumin.* **1977**, *15*, 91.
(38) Janowski, A.; Rzeszotarska, J. *J. Lumin.* **1980**, *21*, 409.
(39) Okuyama, K. hasegawa, T.; Ito, M.; Mikami, N. *J. Phys. Chem.* **1984**, *88*, 1711.
(40) Mondal, J. A.; Ghosh, H. N.; Mukherjee, T.; Palit, D. K. *J. Phys. Chem. A* **2005**, *109*, 6836.
(41) Lewanowicz, A.; Lipiñski, J. *J. Mol. Struct.* **1998**, *450*, 163.
(42) Atom, Y. W.; Robert, H.; Lewis, J. W.; Zangh, J. Z.; Klinger, D. S. *J. Phys. Chem. A* **1999**, *103*, 2388.
(43) Szymanski, M.; Maciejewski, A.; Kozlowski, J.; Koput, J. *J. Phys. Chem. A* **1998**, *102*, 677.
(44) Strickler, S. J.; Berg, R. A. *J. Chem. Phys.* **1962**, *37*, 814.
(45) Grabowski, Z. R.; Rotkiewicz, K.; Rettig, W. *Chem. Rev.* **2003**, *103*, 3899.
(46) Glassbeek, M.; Zhang, H. *Chem. Rev.* **2004**, *104*, 1929.
(47) Riddick, J. A.; Bunger, W. B. *Organic Solvents*, 3rd ed.; Wiley: New York, 1970. The viscosity values at 298 K.